Magnetically actuated rod-shaped nanoswimmers

Jordán Vila Figueirido
Pietro Tierno & José García-Torres, Departament de Física de la Matèria Condensada, Institut de Nanociència i Nanotecnologia, Universitat de Barcelona, Barcelona, Spain

***Abstract*—The idea of creating and controlling very small autonomous devices or nanorobots, which are able to move and operate at such very small scales looks like science fiction. However, this idea may not be that far, many nanoswimming devices are being developed and the challenges of the propulsion in liquid environments at low Reynolds conditions are being overcome. Here, two types of magnetic nanorod-shaped nanoswimmers are realized, one consists only on a nickel nanorod and the other is a nickel-polypyrrole bi-segment nanorod. These nanorods have been actuated using oscillating and rotating magnetic fields and two main types of propulsion mechanisms have been reported, surface walking and flexible undulatory propulsion. An effective control of their speed and direction has been demonstrated and high swimming velocities have been achieved (above 100 μm/s for Ni nanorods).**

***Index Terms*— 4. Nanomagnetism, nanoelectronics and nanophotonics: nanorod, nanoswimmer, magnetic propulsion, surface walker, flexible propeller.**

I. Introduction

Many types of micro- and nanoswimmers have been developed recently and are being investigated because of their promising applications in fields like biomedicine (e.g. drug or gene delivery [1], microsurgery or cell manipulation [2]), environmental remediation (e.g. controlled water decontamination [3]) or nanoengineering (e.g. cargo transport for nanofabrication, or new lithographic techniques [4]), where they can perform tasks at very small scales. These devices can be propelled in different liquid environments and, in some cases, in a controlled way. They can be classified depending on the propulsion mechanisms into: (i) chemical propulsion (e.g. decomposition of H_2O_2 into H_2 [5] or self-electrophoresis [6]), (ii) external stimuli propulsion (magnetic or electric fields [7], light [8] or ultrasounds [9]) or (iii) biological propulsion (e.g. biohybrid micro/nanomotors [10]).

Among the different modes of propulsion, magnetic actuation has been widely used and has several advantages, the fact that these nanoswimmers do not require a chemical reaction makes them more biocompatible and appropriate for biomedical applications. In addition, they can be actuated remotely in an easier way. The most common types of magnetic swimmers by propulsion mechanisms include helical rotating propellers [11], flexible undulatory propellers [12] and 'surface walkers' [13], the last two are the ones studied in this work.

Locomotion at nanoscale is a challenging task due to the low Reynolds number conditions in small systems, where the viscous forces dominate over inertial forces. At these conditions, reciprocal motion movements, e.g. a periodic back and forward body displacement, normally used at larger scales are not valid anymore because of the time reversible nature of the flow, this is known as the '*scallop theorem*' [14]. Furthermore, at these scales the Brownian motion is also dominant and has to be overcome. The locomotion strategies developed are based on breaking the spatial symmetry and time reversibility of the movements. For example, in the case of the helical propellers (inspired by prokaryotic flagella) it is achieved due to their asymmetric shape and the corresponding asymmetry in the friction experienced when actuated by an external rotating field, in flexible propellers (inspired by eukaryotic flagella, like the sperm tail) it is done thanks to the deformations produced in the body or tail. Finally, in the case of surface walkers the symmetry is broken by the rotational-translational coupling, since the swimmer is placed near a surface.

In this work, we report the preparation and characterization of two different types of magnetic nanostructures −single nickel nanorods (Ni NRs) and bi-segmented nickel-polypyrrole nanorods (Ni-PPy NRs) − and study how the NR structure and the magnetic field can affect the mechanism of motion. These nanorods were synthetized by an electrodeposition process. Both types of NRs can act as 'surface walkers', whereas the Ni-PPy NRs can also act as flexible propellers due to the flexible polypyrrole segment.

The nanoswimmers were propelled in a fluid upon application of external oscillating or rotating magnetic fields that apply a torque to the nanorod. From image analysis, we characterize the swimmer velocities by varying the external field parameters, namely the amplitude and frequency of the applied field. When the NRs act as surface walkers they are placed close to a surface and a circular or elliptical rotating magnetic field is applied in a vertical plane, the NRs try to follow it. In the case of the flexible propellers, we apply an oscillating magnetic field along one direction plus a constant component along the perpendicular one and then the nanoswimmer follows the movement in a fish-like way, being propelled by its deformation [12, 15].

These techniques will allow a direct control of speed and direction making them very appropriate for the applications stated before.

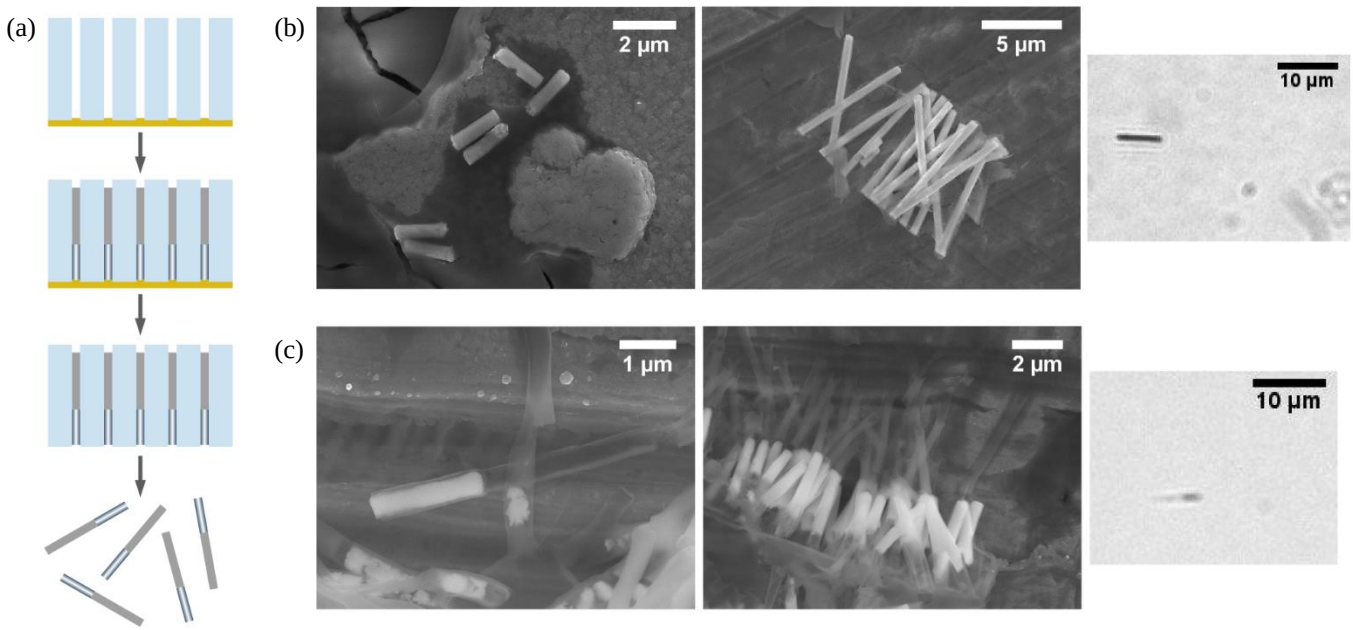

Fig. 1. *Synthesis and structural characterization of the swimmers. (a) Schematic of the template-assisted synthesis of the nanorods shown in three steps: sequential electrodeposition of nickel and polypyrrole in the membrane, etching of the sputtered Au layer and dissolution of polycarbonate membrane. (b) Two SEM images of two groups of Ni nanorods made by electrodeposition with different sizes, and an optical microscope image of one isolated Ni nanorod. (c) Two SEM images of Ni-Polypyrrole nanorods made by electrodeposition, one of an isolated nanorod, a collection of nanorods, and an optical image of one of these nanorods.*

II. Results and Discussion

A. *Nanoswimmers: Synthesis and structural characteristics*

Two main types of nanoswimmers have been fabricated and studied, both of them with a cylindrical shape. The first type, and also the simplest one, consists only of a solid nickel nanorod of around 400 nm diameter and a variable length. The second type has the same shape but it is composed of two materials, so that the nanorod is separated into two segments, one made of nickel and the other made of polypyrrole, which is a conductive flexible polymer whose ability to be deformed will be key for one of the propulsion mechanisms presented. The diameter of the bi-segmented nanorods is also about 400 nm and the lengths of the two parts are variable.

The nanorods have been synthetized by a template-assisted electrodeposition (Fig. 1(a)), in a similar way to [16]. The NRs have been electrodeposited in a polycarbonate membrane as template characterized by holes of about 400 nm. Previously, the membranes have been sputtered in one side with a very thin Au layer which acted as an electrode for the reaction. After the deposition, the Au layer was removed and the polycarbonate membrane was also dissolved, releasing the target nanorods. Finally, these nanorods were dispersed in ultra-pure water, which was used as dispersing medium for propulsion.

In the Fig. 1(b, c) there are two SEM images of each type of nanorod and also on the right side two optical images to show their morphology under an optical microscope. It can be appreciated clearly the solid nickel parts which look brighter in the SEM images due to the higher interaction of the electrons than the polypyrrole, meanwhile they look darker at the optical microscope due to the higher reflectivity of the metals with respect to polymers. In the SEM images from the Ni NRs in Fig. 1(b), diameters between 0.45 – 0.48 µm and lengths between 1.7 – 8 µm have been measured. The diameter is quite homogeneous among the synthetized NRs, meanwhile the lengths vary rather broadly, this may be due to the differences in conductivity in the Au electrode along its surface during electrodeposition. In the bi-segment NRs shown in Fig. 1(c), diameters of about 0.45 µm and lengths between 2 – 2.5 µm have been measured for the Ni segments, and diameters about 0.4 µm and lengths between 3 – 4.5 µm for the PPy segments.

In addition, to the nanorods synthetized by our own, we have also used Ni-PPy nanorods provided by Dr. Salvador Pané from the IRIS research group at ETH Zurich. The main difference with our bi-segmented NRs is the length of each segment –5 µm Ni, 18 µm PPy– making them interesting for comparison purposes.

B. Magnetic actuation of Ni nanorods

First, we have studied the dynamic behavior of Ni nanorods. Several experiments have been realized by changing the configuration and properties of the applied magnetic field and observing the NRs response under optical microscope (see setup details in the Experimental Section).

Our objective was to achieve a good propulsion performance by using the simplest magnetic field actuation. We have tried three main field configurations: linear oscillating magnetic field in the nanorod plane, circular/elliptical rotating field polarized in a vertical plane (see Fig. 2(c)), and mixed oscillating or 'swinging' field (with a static component and another oscillating component perpendicular to it, see field representation in Fig. 5(b). Among all these configurations only

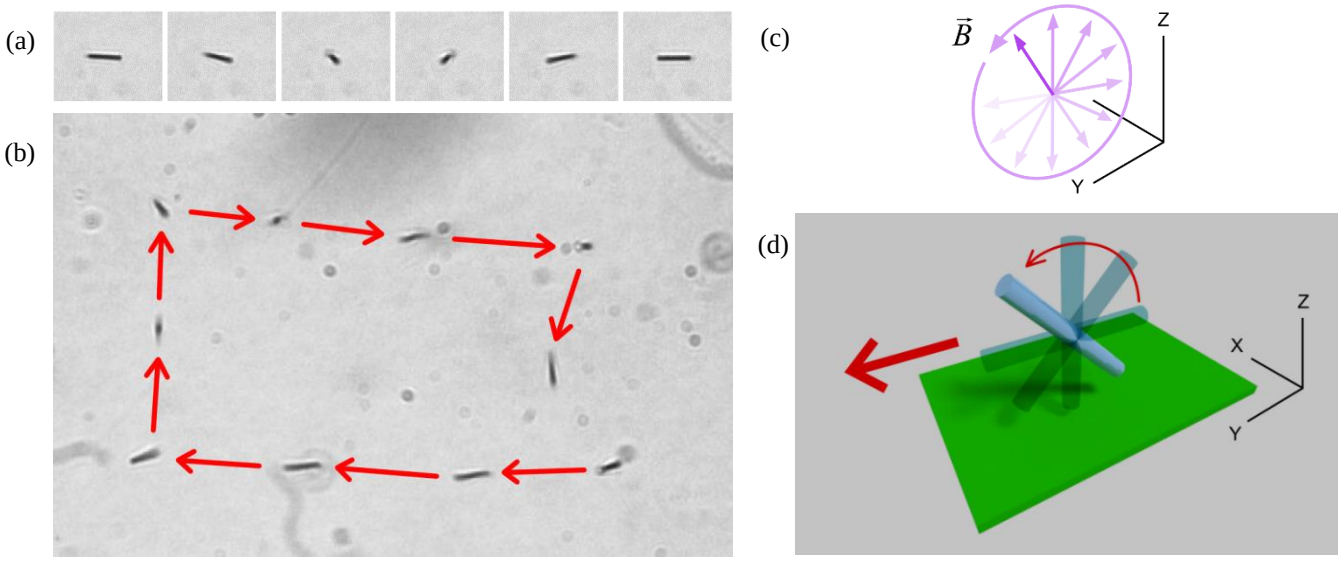

Fig. 2. *Ni nanorods acting as surface walkers. (a) Snapshots from a video of a Ni nanorod being actuated, a half turn is shown. (b) Superposed snapshots from a video showing a Ni surface walker performing a rectangular trajectory. (c) Schematic of the rotating magnetic field (circular in this case). (d) Schematic of the surface walker propulsion mechanism, where the magnetic nanorod spins in a vertical plane following the magnetic field also applied in that spinning direction, this rotation generates different viscous forces in the nanorod end closest to the boundary surface and the other end in the bulk fluid, generating a net displacement.*

the rotating field applied vertically allowed a controllable actuation of the Ni NRs with a net displacement.

For the case of vertical rotating elliptical magnetic field, the horizontal and vertical field components applied were: $B_H = B_{H_0}\sin(2\pi f_r t)$ and $B_V = B_{V_0}\sin(2\pi f_r t \pm \pi/2)$, being B_{H_0} the horizontal and B_{V_0} the vertical amplitudes, and f_r (in turns per second) the rotation frequency. In the case of a circular rotating field, the amplitude B_0 would be equal on both components $B_{H_0} = B_{V_0} = B_0$. Depending on the relative dephasing between the two components ($+\pi/2$ or $-\pi/2$), the field would rotate clockwise or counter-clockwise.

As the nickel nanorods are magnetized along their long axis, they will try to align with the direction of the field. In Fig. 2(a), there are some snapshots of the nanoswimmer motion, where we can observe the vertical rotation of the nanorod. The result of this induced rotation of the nanorod perpendicularly to the surface produces a net displacement in the same direction of the horizontal component of the field. This propulsion mechanism is illustrated in Fig. 2(d), the nanoswimmers that undergo this type of propulsion are usually considered as 'surface walkers'.

The nanorod motion can be explained by considering the effect of the boundary glass plate during the rotation. If the nanorod was actuated by a rotating magnetic field in the bulk fluid (without boundary walls), it would not move in any direction since the magnetic and viscous forces would only affect the angular momentum. The net linear momentum would be null since the rotational motion will produce the same effects along the two directions in one field cycle. However, when the rod is placed near to a surface, there is a difference on the viscous forces acting on the rod ends, the one closest to the plate and the other moving in the bulk. This difference in viscous frictions generates a greater displacement of the free end than the end near the surface, resulting in a net displacement of the rod. Similar approaches of this mechanism of 'surface walker' have been previously reported, for example in Ref. [13], where a colloidal doublet is rotated with a precessing magnetic field, generating a net translational motion.

As it has been shown, changing the rotation direction of the magnetic field, the displacement of the nanorod can be controlled, thus making it a useful mechanism to direct these nanoswimmers at will, at least while they are close to a boundary surface. This latter is shown in Fig. 2(b) where a Ni nanoswimmer has performed a simple rectangular trajectory. Each time the Ni nanorod reaches the corner of the square, the in-plane direction of one component of the applied field is changed in order to make it possible a 90-degree turn.

Now we will see the dynamic characterization of this type of nanoswimmers being actuated by an elliptical magnetic field. In Fig. 3(a), there is a plot of the average speeds of a Ni nanorod of 7.4 μm length being actuated by an elliptical field (whose vertical component is 5 times larger than the horizontal component in all cases) for several values of the rotational frequency and average amplitudes. It can be observed that for all the three amplitudes plotted, there is an almost lineal slope in the lower frequencies until certain 'critical' frequency is reached where this linearity is lost, the velocity decreases as the frequency further increases. This behavior is due to the fact that at lower frequencies the nanorod is still able to follow the rotating magnetic field, and the phase-lag angle between the nanorod and the field is constant. Above the critical frequency, the viscous torque overcome the magnetic one, and the phase-lag angle is not constant anymore. Now the rod is unable to follow the field rotation, its velocity starts to decrease or become unstable. It can be also noticed that the higher is the field amplitude the higher are the frequencies where the linearity is maintained.

Another velocity plot (Fig. 3(b)) has been realized by using a very short Ni NR of about 2.5 μm length. In this case, much higher frequencies have also been applied and some new effects

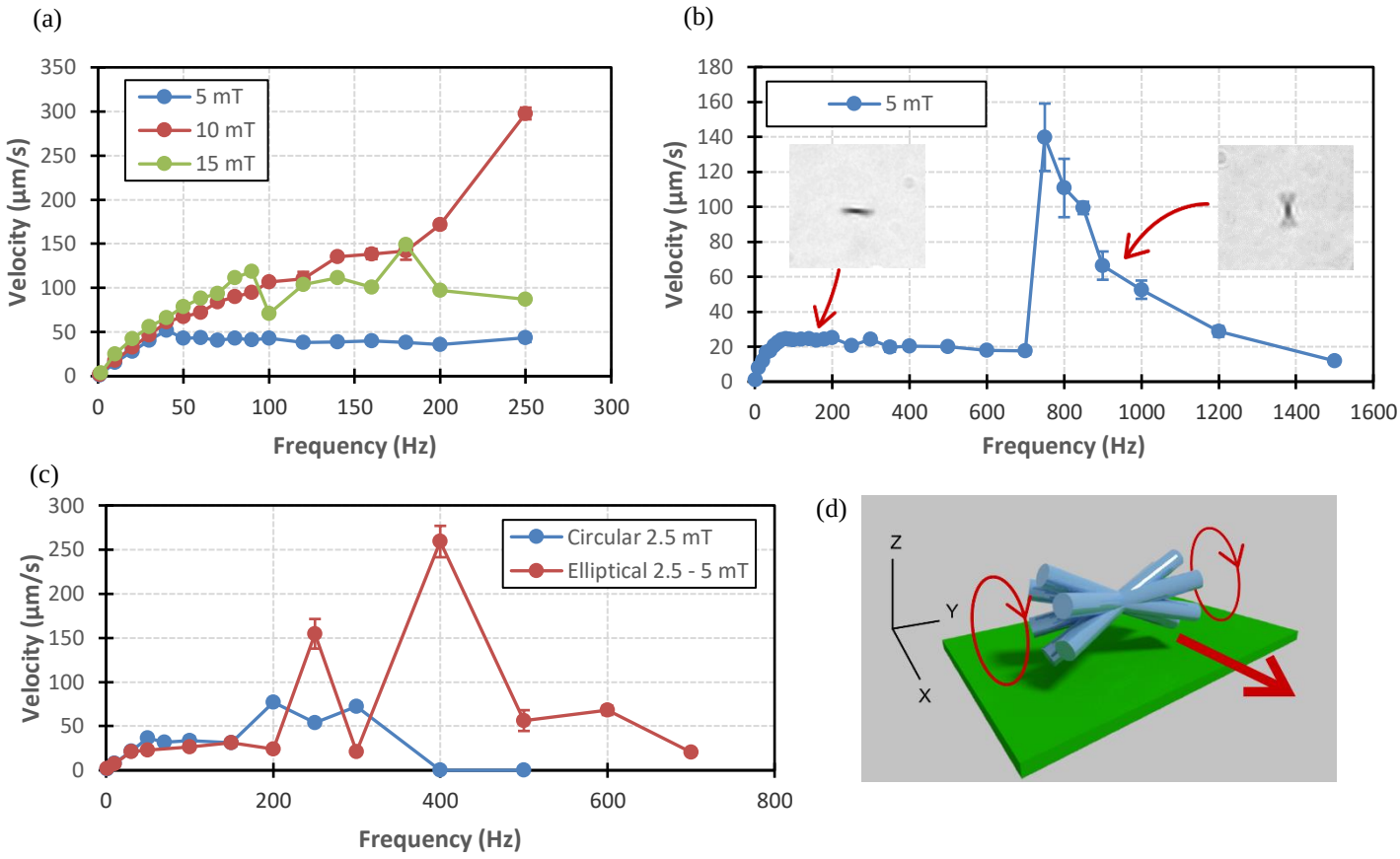

Fig. 3. *Dynamic characterization of Ni nanorods. (a) Average speed as a function of rotation frequency and field amplitude (in mT), the applied magnetic field is elliptical with a relation of 5:1 between the amplitudes of the vertical and horizontal components, the field magnitude shown is an average. Error bars indicate standard deviation of the measurements. (b) Plot of average speed as a function of rotation frequency of a Ni surface walker with an extended range of frequencies to show the extra propulsion modes developed. There are also two snapshots of the two mechanisms observed. (c) Comparison graph showing the average speed as a function of rotation frequency and configuration of magnetic field for a Ni surface walker. In the blue plot a rotating circular magnetic field with equal vertical and horizontal sinusoidal components is applied with a magnitude of 2.5 mT. In the red plot a rotating elliptical field is applied with a vertical component of amplitude 5 mT and a horizontal component of 2.5 mT. (d) Schematic showing a possible 'walking' mechanism with a horizontal 'hourglass' rotating mode with the two ends rotating in parallel planes.*

have been discovered. At the lower range of frequencies (the first 600 Hz) the behavior is very similar as the stated before, with a linear part in the first 50 Hz followed by a slow steady decrease. Apart from this, when very high rotation frequencies where applied, a huge velocity peak was found around 750 Hz with a subsequent exponential decrease. This phenomenon could be explained by a change in the propulsion mechanism, that has been observed in the optical microscope. As it is shown in the optical microscope image on the right in Fig. 3(b), the nanorod here appears to be rotating following a conical precession, where it is laying in horizontal position with both ends spinning in two parallel circles at opposite sides and close to the surface, see Fig. 3(d). This new swimming or walking mechanism is very interesting because higher velocities can be obtained, however, the speed is not lineal with respect to the frequency and also the frequency range where it is produced is variable among the different nanorods and field configurations. This latter, the field configuration effects are demonstrated in the next plot, in Fig. 3(c), where the differences between a circular and elliptical rotating magnetic field (applied to the same nanoswimmer) are shown. During the first 150 Hz the dynamic response is almost the same, still having the lineal part and a slight decay afterwards. Nevertheless, at higher frequencies the difference is more evident, where the elliptical actuation allows higher velocities and the appearance of the new propulsion mechanism.

C. Magnetic actuation of Ni-PPy nanorods

After the characterization of the Ni nanorods, we change the actuation scheme from rotating to oscillating. This change was due to the fact we synthetized bi-segment Ni-PPy nanorods, whose extra segment is made of polypyrrole, a conductive polymer that can be electrodeposited and could introduce flexibility to the nanoswimmer. This extra flexibility would probably break the time-reversible symmetry of the fluid flow under a simple oscillating field, and then generate propulsion.

We have analyzed the actuation response of the Ni-PPy nanorods synthetized, with lengths of up to 2.5 µm for Ni segments and 5 µm for PPy segments. First, several field protocols were used, including simple fields oscillating along one direction, or different combination of static fields and fields oscillating along the perpendicular direction, as shown in Fig. 5(b)). However, we did not observe a net coherent displacement in any of these configurations, in some cases movement was

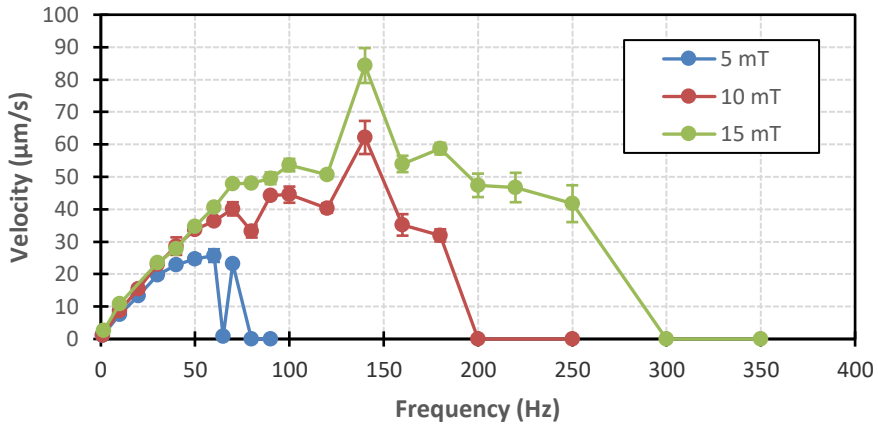

Fig. 4. *Dynamic characterization a Ni-PPy nanorod acting as a surface walker: average speed as a function of rotation frequency and field amplitude (in mT), the applied magnetic field is elliptical with a relation of 5:1 between the amplitudes of the vertical and horizontal components, the field magnitude shown is an average.*

observed but it was always not reproducible, and was probably generated by field inhomogeneities. This absence of motion may be due to a too short PPy tail, whose flexibility at these lengths (5 µm) is not enough to generate propulsion.

Despite the absence of motion with oscillating magnetic fields, the use of rotating vertical fields was also effective with this type of swimmer. In the Fig. 4 there is a graph of an experiment that was conducted under similar field conditions that the one done for the Ni nanorod, but in this case a bi-segment Ni-PPy nanorod has been used (with lengths of 2.3 µm for Ni and 4.7 µm for PPy). It can be observed that the behavior is alike at lower frequencies, the plots have a first linear slope until the critical frequency is reached, and after that the rotation would not be followed synchronously, but then a non-lineal growing tendency is produced and finally a drastic drop of the speed until the nanoswimmer stops totally. The differences are related with the extra flexible PPy segment, that may increase the overall viscous friction and makes it difficult to maintain the motion. In addition, the appearance of other swimming or 'walking' modes at high frequencies above the critical point, that were possible in Ni NRs, may not be viable with the extra PPy segment.

D. Magnetic actuation of Ni-PPy nanorods from IRIS research group

In order to compare different ferromagnetic nanorods, we have also used the Ni-PPy nanorods provided by Dr. Salvador Pané from the IRIS research group at ETH Zurich. Their nanorods have quite higher segment lengths, specially the PPy (about 5 µm Ni and 18 µm PPy).

We have repeated the same dynamic experiments as with our bi-segment nanorods, and in this case, when applying the 'swinging' oscillating magnetic field, a coherent displacement was observed. The extra length of the PPy tail, which allowed more flexibility, was a key point to achieve propulsion. These nanorods were actuated using a planar 'swinging' magnetic field parallel to the glass plate (see Fig. 5(b)), generated in the X and Y axes (magnetic setup details in Experimental Section). A simple approach was realized by applying an oscillating sinusoidal magnetic field in the Y axis and a constant field in the X axis, that would be: $B_X = k$, and $B_Y = B_{Y_0}\sin(2\pi f_r t)$, being k a constant field amplitude, f_r the oscillation frequency (turns per second) and B_{Y_0} the amplitude of the field in the Y axis. Depending on the direction of the applied fields and the oscillation amplitude the nanoswimmer speed and direction can be controlled. When applying the magnetic field, a torque is transmitted to the Ni head and the flexible Ppy tail suffers periodic mechanical deformations that produce a thrust (Fig. 5(c)). Fig. 5(a) illustrate the mechanism of motion of one of these flexible nanoswimmers via a sequence of microscope images, where it can be appreciated that the Ni head tries to align with the applied field continuously while the PPy tail presents an undulating movement. As we have mentioned in the introduction, due to the very low Reynolds number conditions, it is necessary to break the spatial symmetry and the time reversibility of the movements, this is achieved thanks to the PPy bending, where the symmetry is broken. This mechanism has been previously stated by other works, for example in [12] and [15], and these type of nanoswimmers are usually considered flexible propellers.

Now we will see in detail the dynamic response of these Ni-PPy nanoswimmers acting as flexible propellers. In the experiments realized, different frequencies of oscillation have been applied and also different magnitudes of static component (along the X axis) and oscillating component (along the Y axis) were applied, the results are shown in Fig. 5(d). The behavior here has some similarities to the one of surface walkers, there is a first velocity increase at very low frequencies, followed by a velocity decrease until almost stopping. However, the initial increase is much less lineal and the frequencies of dynamic actuation are in general quite lower. The effects of the increase of the oscillation amplitude (field in the Y axis) are clearly seen, the average speeds are raised almost proportionally. Meanwhile the increase of the static field (field in the X axis), in general means a reduction of average speed with respect to the same Y field amplitudes. This may be due to the fact that the ratio between oscillating and static field components, which determines the oscillation angle, may be more determinant than the overall amplitude increase.

Although in our case we have propelled the nanoswimmers

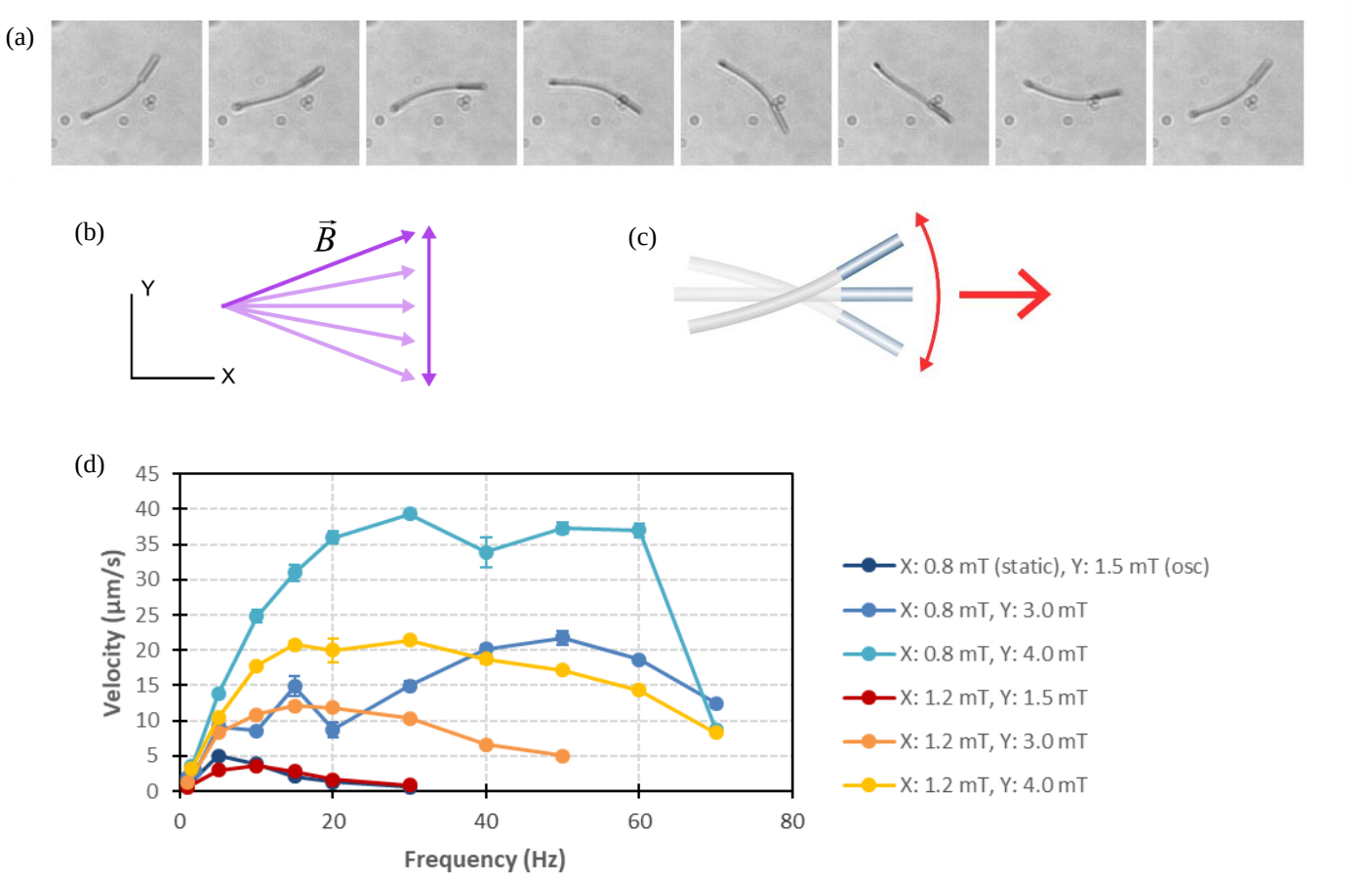

Fig. 5. *Ni-PPy nanorods acting as flexible propellers. (a) Snapshots of a flexible Ni-PPy propeller realizing a complete swimming 'stroke'. (b) Schematic of the 'swinging' field actuation. (c) Schematic of the bi-segment nanorod motion. (d) Average speed as a function of oscillation frequency and magnetic field applied, the field has a static component in the X axis and an oscillating sinusoidal field in the Y axis.*

just above a surface, this mechanism would also be effective without a boundary surface, allowing 3D displacements through the bulk liquid.

E. Final discussion

Making a summary of the performance of all the studied nanoswimmers, we can state that all of them achieved quite high average speeds, that can be precisely controlled by tuning the field frequency. Average speeds of over 100 μm/s can be obtained with Ni surface walkers or over 50 μm/s with Ni-PPy surface walkers, and velocities near 40 μm/s have been obtained with the Ni-PPy flexible propellers.

One advantage of surface walkers is that they can achieve higher velocities than flexible propellers, and they have also a more predictable linear behavior at lower frequencies, meanwhile the main advantage of the flexible propellers is that they use a simpler field actuation and do not need a boundary surface to be propelled, thus being able to navigate in 3D inside the bulk liquid.

III. Conclusion

Two types of rod-shaped nanoswimmers have been fabricated, nanorods composed of only Ni and Ni-PPy. They have been actuated magnetically and two main propulsion mechanisms have been identified: 'surface walking' (in both types) and flexible propulsion mechanisms (only in the longest Ni-PPy NRs). Their dynamic behavior has been successfully studied by changing the frequency and amplitude of the applied field, and a very good performance of the nanoswimmers has been demonstrated, velocities of above 100 μm/s have been achieved for Ni NRs acting as surface walkers and close to 40 μm/s for the Ni-PPy NRs acting as flexible propellers. The direction and magnitude of the speed can be controlled efficiently and this can lead to the development of promising practical applications ranging from the biomedical field to nanoscale manipulation.

IV. Experimental Section

A. Synthesis and preparation of nanoswimmers

Both nickel nanorods (Ni NRs) and bi-segment nickel-polypyrrole nanorods (Ni-PPy NRs) have been synthetized via template-assisted electrodeposition, and in the second case the process involved sequential depositions. The NRs were deposited in a polycarbonate (PC) membrane (from Millipore) with holes having 400 nm diameter. Before these operations, the membrane was sputtered on one side with a thin Au layer, which would be used as working electrode. The counter electrode used was a platinum foil and the reference electrode

was Ag/AgCl/KCl 3M. The obtained diameter of the NRs was about 400 nm or slightly larger, matching the holes of the membrane, and the length was varied by changing the electrodeposition time. The Ni NRs and the Ni segments were electrodeposited by chronoamperometry with a potential of -1.1 V and the plating solution used was 0.1 M $NiCl_2$ (Sigma Aldrich). The polypyrrole segment was electrodeposited just after the Ni segment, such that it grew on top of it. We note that this polymer can be grown by electrodeposition because it is conductive. This segment was electrodeposited by cyclic voltammetry with voltages between -0.3 V and 0.6V, and the plating solution used was 0.01 M pyrrole. The equipment and software used for the electrodeposition was: a potentiostat PGSTAT204 from Autolab and the Nova 2.0 software.

Once the deposition of the NRs was finished, they were released from the membrane. Firstly, the gold layer was removed with a I_2/I^- saturated solution, and subsequently the membrane was dissolved with chloroform ($CHCl_3$). The nanorods were then washed several times in ultrasonic baths with chloroform (15 times), chloroform-ethanol mixture (3 times), ethanol (2 times), and finally rinsed in ultrapure deionised water (2 times). A surfactant, sodium dodecyl sulfate (SDS), was added to the NRs dispersions to reduce the aggregation of the nanorods.

The structure and morphology of the NRs were studied by scanning electron microscopy (SEM).

B. Setup and dynamic analysis

The external field used to induce the propulsion of the nanoswimmers was generated by four custom-made coils of ~1100 turns that realize a triaxial coil system, and which is able to generate a variable field in all three spatial directions. Three of the coils are used to generate the field in X-Y horizontal plane, two of them facing each other in the X axis and the third in the Y axis. The last coil is put below the sample space directed upwards in the Z axis. The coils are connected to a wave generator (TGA1244, TTi) fed by a power amplifier (IMG AMP-1800). When a constant magnetic field was needed the coils of the X axis were connected to a DC power supply. For the calibration of the magnetic field intensities a teslameter (FM 205, ProjektElektronik GmbH) was used. All the coils were arranged on the stage of a light microscope (Eclipse Ni, Nikon), and the nanoswimmers behavior was recorded with charge coupled device cameras working at 75 fps (scA640-74fc, Basler) or 500 fps (acA640-750uc, Basler) for the high-speed videos.

ACKNOWLEDGMENT

J.V. thanks the research group of Magnetic Soft Matter in Universitat de Barcelona, with a special mention to Dr. José García Torres and Dr. Pietro Tierno for their guidance and supervision throughout the experimental procedures and writing of the manuscript. The authors thank Dr. Salvador Pané from the IRIS research group at ETH Zurich for providing the long Ni-PPy nanorods that they had synthetized. J.V. also thanks the Chemist Claudia García Mintegui for her contributions to improve the manuscript and for her pleasant company in the laboratory. Finally, J.V. also thanks the Physicist Alberto Saavedra García and the Engineer Miguel Aguilar Moreno for their unconditional support.

REFERENCES

[1] Qiu, F., Fujita, S., Mhanna, R., Zhang, L., Simona, B.R. & Nelson, B.J. 2015, "Magnetic Helical Microswimmers Functionalized with Lipoplexes for Targeted Gene Delivery", *Advanced Functional Materials*, vol. 25, no. 11, pp. 1666-1671.

[2] Xi, W., Solovev, A.A., Ananth, A.N., Gracias, D.H., Sanchez, S. & Schmidt, O.G. 2013, "Rolled-up magnetic microdrillers: Towards remotely controlled minimally invasive surgery", *Nanoscale*, vol. 5, no. 4, pp. 1294-1297.

[3] Guix, M., Orozco, J., Garcia, M., Gao, W., Sattayasamitsathit, S., Merkoči, A., Escarpa, A. & Wang, J. 2012, "Superhydrophobic alkanethiol-coated microsubmarines for effective removal of oil", *ACS Nano*, vol. 6, no. 5, pp. 4445-4451.

[4] Li, J., Gao, W., Dong, R., Pei, A., Sattayasamitsathit, S. & Wang, J. 2014, "Nanomotor lithography", *Nature Communications*, vol. 5.

[5] Gibbs, J.G. & Zhao, Y.-P. 2009, "Autonomously motile catalytic nanomotors by bubble propulsion", *Applied Physics Letters*, vol. 94, no. 16.

[6] Paxton, W.F., Baker, P.T., Kline, T.R., Wang, Y., Mallouk, T.E. & Sen, A. 2006, "Catalytically induced electrokinetics for motors and micropumps", *Journal of the American Chemical Society*, vol. 128, no. 46, pp. 14881-14888.

[7] Loget, G. & Kuhn, A. 2011, "Electric field-induced chemical locomotion of conducting objects", *Nature Communications*, vol. 2, no. 1.

[8] Dai, B., Wang, J., Xiong, Z., Zhan, X., Dai, W., Li, C.-, Feng, S.-. & Tang, J. 2016, "Programmable artificial phototactic microswimmer", *Nature Nanotechnology*, vol. 11, no. 12, pp. 1087-1092.

[9] Wang, W., Duan, W., Zhang, Z., Sun, M., Sen, A. &Mallouk, T.E. 2015, "A tale of two forces: Simultaneous chemical and acoustic propulsion of bimetallic micromotors", *Chemical Communications*, vol. 51, no. 6, pp. 1020-1023.

[10] Magdanz, V., Sanchez, S. & Schmidt, O.G. 2013, "Development of a sperm-flagella driven micro-bio-robot", *Advanced Materials*, vol. 25, no. 45, pp. 6581-6588.

[11] Gao, W., Feng, X., Pei, A., Kane, C.R., Tam, R., Hennessy, C. & Wang, J. 2014, "Bioinspired helical microswimmers based on vascular plants", *Nano Letters*, vol. 14, no. 1, pp. 305-310.

[12] Li, T., Li, J., Zhang, H., Chang, X., Song, W., Hu, Y., Shao, G., Sandraz, E., Zhang, G., Li, L. & Wang, J. 2016, "Magnetically Propelled Fish-Like Nanoswimmers", *Small*, vol. 12, no. 44, pp. 6098-6105.

[13] Tierno, P., Golestanian, R., Pagonabarraga, I. &Sagués, F. 2008, "Magnetically actuated colloidal microswimmers", *Journal of Physical Chemistry B*, vol. 112, no. 51, pp. 16525-16528.

[14] Purcel, E.A. 1977, "Life at low Reynolds number", *American Journal of Physics*, vol. 45, no. 1, pp. 3-11.

[15] Jang, B., Gutman, E., Stucki, N., Seitz, B.F., Wendel-García, P.D., Newton, T., Pokki, J., Ergeneman, O., Pané, S., Or, Y. & Nelson, B.J. 2015, "Undulatory Locomotion of Magnetic Multilink Nanoswimmers", *Nano Letters*, vol. 15, no. 7, pp. 4829-4833.

[16] García-Torres, J., Calero, C., Sagués, F., Pagonabarraga, I. &Tierno, P. 2018, "Magnetically tunable bidirectional locomotion of a self-assembled nanorod-sphere propeller", *Nature Communications*, vol. 9, no. 1.